Journal of Alloys and Compounds 509 (2011) 4613–4616

Contents lists available at ScienceDirect

Journal of Alloys and Compounds

journal homepage: www.elsevier.com/locate/jallcom

Magnetic and magnetocaloric properties of ternary Gd–Co–Al bulk metallic glasses

H. Fu[a,b,*], M. Zou[b]

[a] Department of Applied Physics, University of Electronic Science and Technology of China, Chengdu 610054, PR China
[b] The Ames Laboratory, U.S. Department of Energy, Iowa State University, Ames, Iowa 50011-3020, USA

ARTICLE INFO

Article history:
Received 18 July 2010
Received in revised form 9 December 2010
Accepted 19 January 2011
Available online 26 January 2011

Keywords:
Rare earth
Bulk metallic glass
Magnetocaloric effect

ABSTRACT

Bulk metallic glasses (BMGs) with compositions of $Gd_{55}Co_xAl_{45-x}$ ($15 \le x \le 30$) and $Gd_{60}Co_yAl_{40-y}$ ($15 \le y \le 30$) were synthesized by an injection casting technique. Temperature dependence of magnetization of the BMGs indicates that their Curie temperatures can be tailored between 96 and 143 K by varying Gd and Co concentration. The magnetic entropy changes of the BMGs are greater than 9.0 J/kg K except for the $Gd_{55}Co_{30}Al_{15}$ glass that exhibits a reduced magnetization due to its large Co content. The relative cooling powers of the BMGs are greater than those of any other crystalline compounds and decrease with the increasing Co content.

1. Introduction

Materials exhibiting magnetocaloric effect (MCE) for magnetic refrigeration applications are one of the hottest topics in the applied physics field in the last decade [1]. The heavy rare earth based BMGs bearing large MCE at different temperatures are promising candidates for magnetic refrigerants [2–4]. Among them, Gd-based amorphous alloys possessing good glass-forming ability (GFA) and relative cooling power (RCP) without any hysteresis loss have attracted special attention. For example, the $Gd_{52.5}Co_{16.5}Al_{31}$ BMG possesses a critical casting diameter of 4 mm, magnetic entropy change of 9.8 J/kg K (upon 0 to 50 kOe field change), and RCP of 9.1×10^2 J/kg [5].

To date, the knowledge of how the composition affects the magnetic and magnetocaloric properties of ternary Gd–Co–Al BMGs is still absent. Here we present a preliminary investigation on the composition dependence of Curie temperature, Co moment, and magnetocaloric effect at the Gd-rich end of ternary Gd–Co–Al BMGs. Two alloy series with composition of $Gd_{55}Co_xAl_{45-x}$ ($15 \le x \le 30$) and $Gd_{60}Co_yAl_{40-y}$ ($15 \le y \le 30$) were selected for the study. The reason is that these alloys exhibited good GFA and formed glass rods with a diameter exceeding 2 mm by an injection casting technique [6,7].

2. Experimental

The $Gd_{55}Co_xAl_{45-x}$ ($15 \le x \le 30$) and $Gd_{60}Co_yAl_{40-y}$ ($15 \le y \le 30$) BMGs were synthesized by injection casting. Every Gd–Co–Al master alloy, ~3 g, with varied nominal composition listed in Table 1, was prepared by arc-melting pure Al (99.99 wt.%), Co (99.9 wt.%), and Ames Laboratory high purity Gd (99.9 at.%) [8] in a Zr-gettered argon atmosphere. The ingots were repeatedly melted for at least four times to ensure homogeneity. The weight loss of the samples after melting is smaller than 0.1%. The square cuboid-shaped samples with a length of about 30 mm and a cross section side length of 1 mm were formed by injecting the molten metal into copper molds with cavities. The phase purity of the alloy buttons was verified by powder X-ray diffraction (XRD) using a PANatytical X'pert Pro diffractometer with a Cu $K\alpha_1$ radiation. Long count time of 600 s/step was employed to obtain data with good signal-to-noise ratios. The temperature and field dependencies of magnetization were measured by using a superconducting quantum interference device (SQUID) magnetometer, model of MPMS XL-7.

3. Results and discussion

Fig. 1 shows the XRD patterns of $Gd_{55}Co_xAl_{45-x}$ [$10 \le x \le 30$, Fig. 1(a)] and $Gd_{60}Co_yAl_{40-y}$ [$15 \le y \le 30$, Fig. 1(b)] BMGs. The peak at 26.7° is the strongest peak of SiO_2 (PDF2-03-065-0466) mortar contamination due to the superior hardness of the BMGs. The absence of Bragg peaks indicates that the samples are topological disordered within XRD resolution.

The temperature dependence of magnetization with a 0.1 kOe applied magnetic field for $Gd_{55}Co_xAl_{45-x}$ ($15 \le x \le 30$) and $Gd_{60}Co_yAl_{40-y}$ ($15 \le y \le 30$) glass alloys are shown in Fig. 2(a) and (b), respectively. For all the samples, a sharp transition is observed where the magnetization (M) exhibits a dramatic upturn upon cooling through the ordering temperature. The Curie–Weiss fit of the data above the ordering temperature is shown in Fig. 2(c) and (d).

* Corresponding author at: Department of Applied Physics, University of Electronic Science and Technology of China, No. 4, Section 2, North Jianshe Road, Chengdu, Sichuan 610054, PR China.
E-mail address: fuhao@uestc.edu.cn (H. Fu).

0925-8388/$ – see front matter © 2011 Elsevier B.V. All rights reserved.
doi:10.1016/j.jallcom.2011.01.126

Table 1
Composition, magnetic, and magnetocaloric properties of $Gd_{55}Co_xAl_{45-x}$ ($15 \le x \le 30$) and $Gd_{60}Co_yAl_{40-y}$ ($15 \le y \le 30$) BMGs.

Composition	T_C (K)	θ_P (K)	P_{eff} (μ_B)	P_{Co} (μ_B)	M_s/f.u. (μ_B)	Co moment (μ_B)[a]	$-\Delta S_{Mmax}$ (J/kg K)	δ_{FWHM} (K)	RCP ($\times 10^2$ J/kg)
$Gd_{55}Co_{15}Al_{30}$	96	110	7.3	4.2	406.5	−0.58	9.4	95.9	9.1
$Gd_{55}Co_{20}Al_{25}$	104	117	7.2	4.6	402.8	−0.62	9.6	88.9	8.5
$Gd_{55}Co_{25}Al_{20}$	114	125	7.0	4.1	402.5	−0.51	9.6	82.4	7.9
$Gd_{55}Co_{30}Al_{15}$	128	137	6.9	4.4	395.3	−0.67	8.6	95.0	8.2
$Gd_{60}Co_{15}Al_{25}$	105	118	7.4	4.6	441.0	−0.80	9.2	97.3	9.0
$Gd_{60}Co_{20}Al_{20}$	112	128	7.3	4.9	440.2	−0.64	9.3	90.1	8.4
$Gd_{60}Co_{25}Al_{15}$	124	136	7.0	3.9	442.6	−0.42	9.3	86.1	8.0
$Gd_{60}Co_{30}Al_{10}$	143	155	6.8	3.6	433.3	−0.66	9.1	83.6	7.6

[a] The minus sign of Co moment indicates the antiparallel alignment of the Gd and Co moments.

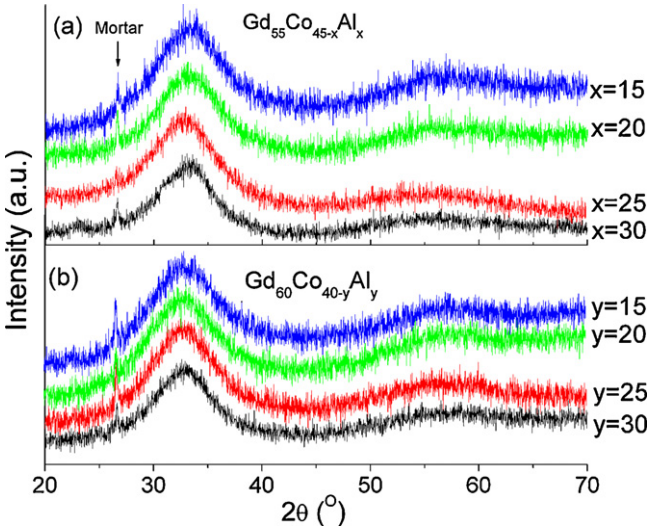

Fig. 1. XRD patterns of $Gd_{55}Co_xAl_{45-x}$ ($15 \le x \le 30$) (a) and $Gd_{60}Co_yAl_{40-y}$ ($15 \le y \le 30$) (b) BMGs.

The Curie temperatures as well as the paramagnetic Curie points, T_Cs and θ_Ps, defined as the temperatures at the maxima of $|dM/dT|$ vs. T and the intercept by extrapolating the linear part of inverse susceptibility at high temperature to abscissa, respectively, are summarized in Table 1. The positive θ_Ps indicates that the predominant exchange interaction in the alloys is ferromagnetic or ferrimagnetic.

The Co content dependence of T_Cs in the two alloy series is plotted in Fig. 3. Obviously, T_Cs increase with the increasing Co content for a specific Gd content, which is due to the strong direct exchange interaction between the Co atoms. The T_Cs can be fitted into:

$$T_{C(Gd55)} = 0.0629x^2 - 0.7143x + 92.8 \quad (1)$$

$$T_{C(Gd60)} = 0.0973y^2 - 1.8366y + 110 \quad (2)$$

for the two alloy series. On the other hand, for a specific Co content, the T_C increases by ~10 K when Gd content increases from 55% to 60 at.%, i.e. T_C increases with increased Gd content at a rate of ~2 K per at.%. This increase can be attributed to the higher T_C (~250 K) of amorphous Gd metal [9]. Therefore, the Curie temperature can be tailored via both Gd and Co concentrations for these BMGs. The maximum T_C is 143 K in $Gd_{60}Co_{30}Al_{10}$ for the two series.

The effective moments per atom (P_{eff}) derived from the Curie–Weiss fits are shown in Table 1. Assuming the effective moment of Gd (P_{Gd}) is 7.94 μ_B, the effective moment of Co (P_{Co}) can be calculated from a weighted average of the form

$$P_{eff}^2 = xP_{Gd}^2 + (1-x)P_{Co}^2 \quad (3)$$

where x represents the concentration of Gd in the magnetic species [10]. The calculated P_{Co} varies between 3.6 and 4.9 μ_B, which is close to 3.87 and 4.90 μ_B, calculated from $P = 2\sqrt{S(S+1)}$ for the free Co^{2+} and Co^{3+} ions, respectively [11]. Therefore, the Co ions reserve their localized spin moments even at a low Co content as 15 at.%.

Magnetization isotherms of $Gd_{55}Co_{15}Al_{30}$ glass measured at temperatures between 2 and 180 K with applied fields between 0 and 50 kOe are shown in Fig. 4. The magnetic hysteresis is negligible at all measured temperatures. The magnetization measured at 2 K is easy to saturate when the applied field is greater than 10 kOe. This feature indicates that $Gd_{55}Co_{15}Al_{30}$ glass orders ferromagnetically or ferrimagnetically with a collinear structure. Extrapolating the 2 K magnetization to $1/H = 0$ results in a saturation magneti-

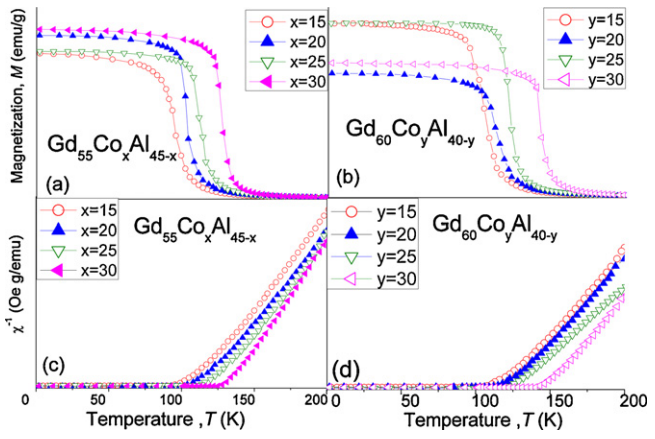

Fig. 2. Temperature dependencies of magnetization of $Gd_{55}Co_xAl_{45-x}$ ($15 \le x \le 30$) (a) and $Gd_{60}Co_yAl_{40-y}$ ($15 \le y \le 30$) (b) BMGs measured with a 0.1 kOe applied field upon cooling. The inverse susceptibility derived from (a) and (b) are shown in (c) and (d), respectively.

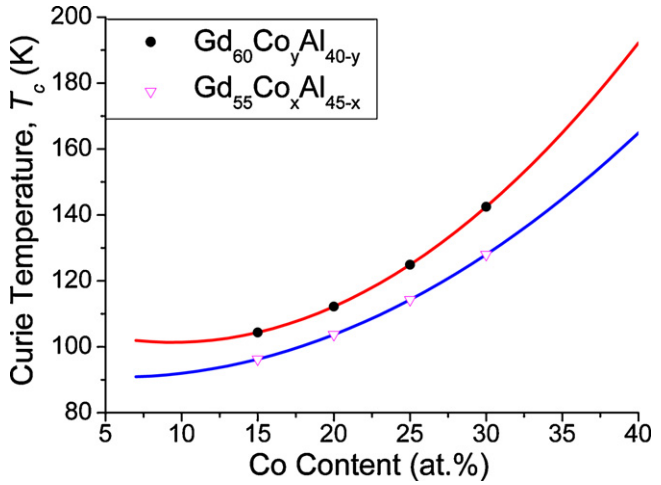

Fig. 3. The dependence of Curie temperatures on Co content of $Gd_{55}Co_xAl_{45-x}$ ($15 \le x \le 30$) and $Gd_{60}Co_yAl_{40-y}$ ($15 \le y \le 30$) alloy series.

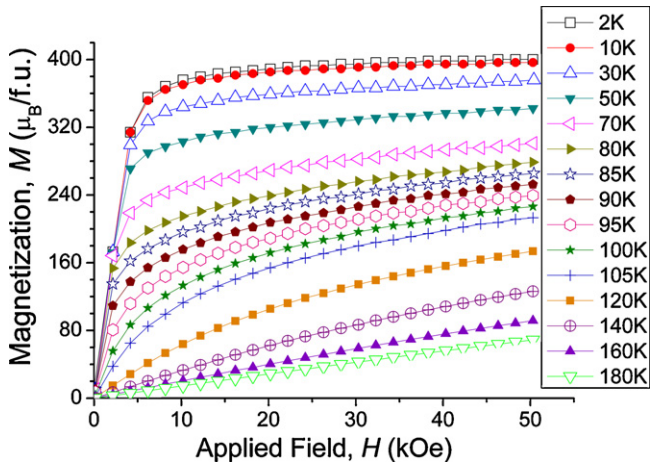

Fig. 4. Magnetization isotherms of $Gd_{55}Co_{15}Al_{30}$ at temperatures between 2 and 180 K and with applied fields between 0 and 50 kOe.

zation (M_s) of 406.5 μ_B/f.u. Assuming that the magnetic moment per Gd atom is 7.55 μ_B [12], the average magnetic moment per Co atom is evaluated as −0.6 μ_B, which is smaller than that in the Co metal (~1.7 μ_B). This discrepancy is possibly due to the charge transfer from Gd and/or Al [13]. The saturation magnetizations and moments of Co ions at 2 K for other alloys evaluated by the same method are listed in Table 1. The minus sign indicates the antiparallel alignment between the Gd and Co moments. Therefore, these ternary Gd–Co–Al glasses are likely collinearly ferrimagnetic.

Fig. 5 shows the temperature dependence of magnetic entropy changes calculated using the Maxwell relation for the two alloy series. The maxima of magnetic entropy changes ($-\Delta S_{Mmax}$) are summarized in Table 1. All the magnetic entropy changes are greater than 9.0 J/kg K for $\Delta H = 50$ kOe except for the $Gd_{55}Co_{30}Al_{15}$ glass. According to the Maxwell relation, the magnetic entropy

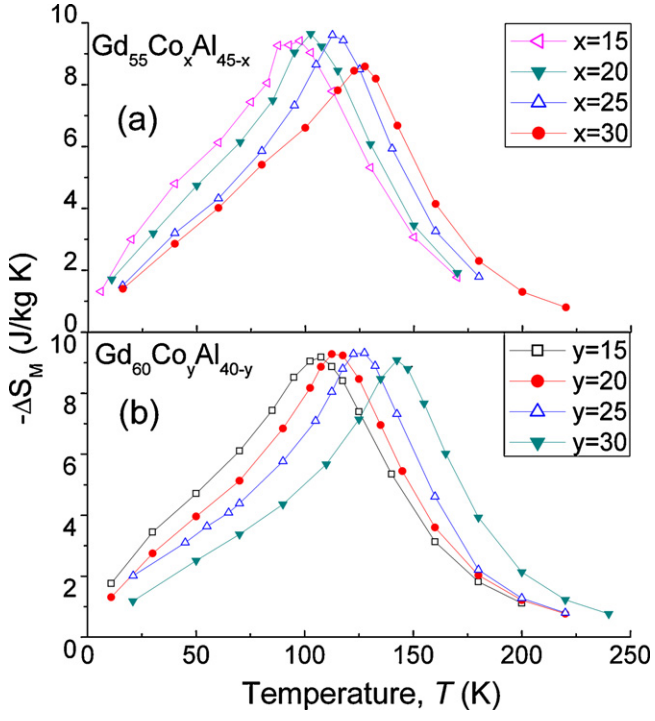

Fig. 5. Temperature dependencies of magnetic entropy changes ($-\Delta S_M$) of $Gd_{55}Co_xAl_{45-x}$ ($15 \le x \le 30$) (a) and $Gd_{60}Co_yAl_{40-y}$ ($15 \le y \le 30$) (b) calculated from the magnetization isotherms for a change in the magnetic field from 0 to 50 kOe.

change depends on the magnetization (M) and its changing rate with temperature, $\left|\partial M/\partial T\right|$. Therefore, the lowest magnetization of $Gd_{55}Co_{30}Al_{15}$ glass due to the increasing of Co content is responsible for its lowest magnetic entropy change in these series. At temperatures near 100 K, there are two types of magnetic refrigerants [14]. The first type is the crystalline compounds exhibiting first order magnetic transition (FOMT) and giant magnetic entropy changes. For example, the magnetic entropy changes of $HoCo_2$ and Gd_5SiGe_3 are 19.7 and 48.8 J/kg K for $\Delta H = 50$ kOe, respectively [14]. The second type is the crystalline compounds having second order magnetic transition (SOMT) such as GdCoAl whose magnetic entropy change is 10.4 J/kg K [15]. Although the magnetic entropy changes of the BMGs in Table 1 are smaller than those with FOMT, they are comparable with those of compounds with SOMT. It is worth noting that the BMGs have the advantage of no thermal or magnetic hysteresis over the compounds with FOMT.

The novel features of the BMGs are the large full width at half maximum (δ_{FWHM}) of the magnetic entropy change curves (see Fig. 5 and Table 1) and the resulting large RCP [16]. All the δ_{FWHM}s are greater than 80 K, which is larger than those of any other crystalline magnetic refrigerants. For example, the δ_{FWHM}s for $MnFeP_{0.45}As_{0.55}$ [17], $Gd_5Si_2Ge_2$ [18], $La(Fe_{0.88}Si_{0.12})_{13}$ [19], MnAs [20], and Gd [17] are 24, 36, 23, 16, and 55 K, respectively. Near 100 K, GdCoAl possesses the largest δ_{FWHM}, 70 K, among the crystalline compounds [15]. However, its δ_{FWHM} and RCP are smaller than those of the BMGs shown in Table 1. Furthermore, it can be seen from Table 1 that the δ_{FWHM}s and RCPs decrease with the increasing of Co concentration except for the $Gd_{55}Co_{30}Al_{15}$ glass. The increase of RCP for the $Gd_{55}Co_{30}Al_{15}$ glass is due to the abnormal increase of δ_{FWHM} due to the decrease in the magnetic entropy change. The large δ_{FWHM}s and RCPs of the BMGs are a result of the distribution of the exchange interactions due to the different exchange integral at different sites with variational distance and bond angle in the topologically disordered structure [21]. Therefore, even far below the measured T_C, some pairs of spins with a lower exchange integral reach their own transition temperatures and align to the magnetic field.

4. Conclusions

The Curie temperatures of Gd-rich Gd–Co–Al BMGs were found to increase with the increasing of Gd and/or Co concentration. The effective moments of Co calculated from Cruie–Weiss fit are close to that of free Co ion, which confirms Co reserves its moment even when its content in the BMGs is as low as 15%. The Gd–Co–Al BMGs are ferrimagnetic and the moment of Co determined from the saturation magnetization at 2 K is about 0.6 μ_B for all investigated alloys assuming the Gd moment is 7.55 μ_B. The magnetic entropy changes of the BMGs are greater than 9.0 J/kg K except for $Gd_{55}Co_{30}Al_{15}$ glass with reduced magnetization due to a high Co concentration. The RCPs of BMGs are greater than those of any other crystalline compounds and decrease with the increasing of Co content.

Acknowledgements

This work was supported by the National Natural Science Foundation of China (No. 50901013). Work at the Ames Laboratory was supported by the U.S. Department of Energy, Office of Basic Energy Sciences, Division of Materials Sciences and Engineering under Contract No. DE-AC02-07CH11358 with Iowa State University of Science and Technology. We acknowledge Drs. K.A. Gshneidner, Jr. and V.K. Pecharsky for their support in sample preparation and characterization.

References

[1] V.K. Pecharsky, K.A. Gschneidner, Phys. Rev. Lett. 78 (1997) 4494.
[2] W.H. Wang, Adv. Mater. 21 (2009) 4524–4544.
[3] Q. Luo, D.Q. Zhao, M.X. Pan, W.H. Wang, Appl. Phys. Lett. 89 (2006) 081914.
[4] Q. Luo, W.H. Wang, J. Non-Cryst. Solids 355 (2009) 759.
[5] H. Fu, M.S. Guo, H.J. Yu, X.T. Zu, J. Magn. Magn. Mater. 321 (2009) 3342–3345.
[6] D. Chen, A. Takeuchi, A. Inoue, Mater. Sci. Eng. A 457 (2007) 226–230.
[7] A. Zhang, D. Chen, Z. Chen, Phil. Mag. Lett. 89 (2009) 59–65.
[8] Materials Preparation Center, Ames Laboratory, US DOE. www.mpc.ameslab.gov.
[9] K. Moorjani, J.M.D. Coey, Magnetic Glasses, Elsevier, Amsterdam-Oxford-New York-Tokyo, 1984, 222.
[10] J.A. Gerber, D.J. Miller, D.J. Sellmyer, J. Appl. Phys. 49 (1978) 1699–1701.
[11] É. du Treĭmolet de Lacheisserie, D. Gignoux, M. Schlenker, Magnetism: Fundamentals Materials and Applications, vol. 1, Kluwer Academic Publishers, 2002, 265.
[12] H.E. Nigh, S. Legvold, F.H. Spedding, Phys. Rev. 132 (1963) 1092–1097.
[13] N. Heiman, N. Kazama, Phys. Rev. B 17 (1978) 2215–2220.
[14] K.A. Gschneidner, V.K. Pecharsky, A.O. Tsokol, Rep. Prog. Phys. 68 (2005) 1479–1539.
[15] X.X. Zhang, F.W. Wang, G.H. Wen, J. Phys.: Condens. Matter 13 (2001) L747–L752.
[16] K.A. Gschneidner, V.K. Pecharsky, Ann. Rev. Mater. Sci. 30 (2000) 387–429.
[17] O. Tegus, E. Bruck, K.H.J. Buschow, F.R. de Boer, Nature 415 (2002) 150–152.
[18] A.O. Pecharsky, K.A. Gschneidner, V.K. Pecharsky, J. Appl. Phys. 93 (2003) 4722–4728.
[19] A. Fujita, S. Fujieda, Y. Hasegawa, K. Fukamichi, Phys. Rev. B 67 (2003) 104416.
[20] H. Wada, T. Morikawa, K. Taniguchi, T. Shibata, Y. Yamada, Y. Akishige, Phys. B 328 (2003) 114–116.
[21] J.M.D. Coey, J. Appl. Phys. 49 (1978) 1646–1652.